Naval Research Laboratory

Washington, DC 20375-5320

NRL/MR/5508--10-9233

Using Morphological Filters for Pupil Detection in Infrared Videos

Haw-Jye Shyu

Information Management and Decision Architecture Branch
Information Technology Division

Roger Hillson

Adversarial Modeling and Exploitation Office
Information Technology Division

January 5, 2010

REPORT DOCUMENTATION PAGE

Form Approved
OMB No. 0704-0188

1. REPORT DATE *(DD-MM-YYYY)* 05-01-2010	**2. REPORT TYPE** Memorandum Report	**3. DATES COVERED** *(From - To)* Jan 2008 - Aug 2008

4. TITLE AND SUBTITLE Using Morphological Filters for Pupil Detection in Infrared Videos	**5a. CONTRACT NUMBER** **5b. GRANT NUMBER** **5c. PROGRAM ELEMENT NUMBER**
6. AUTHOR(S) Haw-Jye Shyu and Roger Hillson	**5d. PROJECT NUMBER** 55-6010 **5e. TASK NUMBER** **5f. WORK UNIT NUMBER**
7. PERFORMING ORGANIZATION NAME(S) AND ADDRESS(ES) Naval Research Laboratory 4555 Overlook Avenue, SW Washington, DC 20375-5320	**8. PERFORMING ORGANIZATION REPORT NUMBER** NRL/MR/5508--10-9233
9. SPONSORING / MONITORING AGENCY NAME(S) AND ADDRESS(ES) Naval Research Laboratory 4555 Overlook Avenue, SW Washington, DC 20375-5320	**10. SPONSOR / MONITOR'S ACRONYM(S)** **11. SPONSOR / MONITOR'S REPORT NUMBER(S)**

12. DISTRIBUTION / AVAILABILITY STATEMENT

Approved for public release; distribution is unlimited.

13. SUPPLEMENTARY NOTES

14. ABSTRACT

Patterns of eye movements may be indicative of a subject's cognitive state, including the likelihood that a subject is lying or telling the truth. Medical systems exist for tracking eye movements, but their use requires artificially constraining head movements in a manner that is incompatible with an interview scenario. The eye movement analysis contained in this report was conducted retroactively, using data collected elsewhere using a simple experimental setup. The subjects were photographed using a single camera equipped with a single IR (infrared) illuminator. A three-stage process of morphological filtering was used to detect the subjects' pupils, with manual parameterization of the filter coefficients. False detections due to background clutter from eyeglasses and jewelry were significantly reduced, but not entirely eliminated. Use of an elliptical filter, rather than a circular filter, improved the outcome for the final stage of pupil detection. Although improved methods exist for reducing false detections, the data collection protocols are far more complex than the single-camera/single-illuminator protocol used here.

15. SUBJECT TERMS

Morphological filtering	Morphological closing	Eye movements	Pupil detection
Morphological opening	Boundary detection	Eye movement tracking	Infrared illumination

16. SECURITY CLASSIFICATION OF:			**17. LIMITATION OF ABSTRACT**	**18. NUMBER OF PAGES**	**19a. NAME OF RESPONSIBLE PERSON**
a. REPORT	**b. ABSTRACT**	**c. THIS PAGE**	UL	16	Roger Hillson
Unclassified	Unclassified	Unclassified			**19b. TELEPHONE NUMBER** *(include area code)* (202) 404-7332

Standard Form 298 (Rev. 8-98)
Prescribed by ANSI Std. Z39.18

Table of Contents

1) Background **1**

2) Approach **2**

a) Thresholding *4*

b) Morphological filtering *5*

c) Fitting the detected objects with ellipses *7*

d) Add image intensity constraints on the detected ellipse *9*

3) Conclusion and Discussion **11**

4) Acknowledgments **12**

5) References **12**

Table of Figures

Figure 1 - Data flow diagram of pupil detection 2
Figure 2 – An original infrared image.......... 3
Figure 3 – The gray version of the original image.......... 3
Figure 4 - A resultant binary image after the thresholding. 4
Figure 5 – A resultant image after the morphological opening process. 6
Figure 6 – A resultant image after the morphological closing process.......... 6
Figure 7 – The detected boundaries overlaid on the original infrared image.......... 7
Figure 8 –Fitting the elongated pupils with circles often failed. 8
Figure 9 – Fitting the elongated pupils with ellipses had a higher successful rate of pupil detection. 8
Figure 10 – Detected ellipses overlaid on the gray scale image. 9
Figure 11 – The detected small ellipse with associated iris area. 10
Figure 12 – The final detected pupils are overlaid on the original IR image. 11

1) Background

Some studies [1, 2] suggest that the pattern of a subject's eye movements may be one indicator of whether a subject is lying or telling the truth. Prior to testing this hypothesis, it is important to develop a real-time, non-invasive automatic eye tracking system to detect and track the eye movements of a subject.

Currently, there are medical systems (video oculography systems) available for patient eye movement tracking. However, these systems are not suitable for our application. To limit the head movement, the video oculography systems typically require that the subject 1) wear a head mounted camera system, 2) restrict his gaze to a very limited space in front of him, or 3) use a chin rest to support his head. For a survey of oculography systems refer to [3].

In contrast to the medical oculography systems, our approach allows the subject a much greater degree of freedom to move and look around. While sitting about eight feet in front of the digital camera, subjects are allowed to move their heads freely and to gaze anywhere they wish. This type of setup is very difficult to achieve with a medical video oculography system. There are many factors that hinder the successful detection and tracking of eye-movement, for example:

- The head movement of a subject - when the subject moves his/her head quickly, it can create a relatively high speed eye movement which can blur the pupil image

- The oblique look directions of the subject - when the subject looks in an oblique direction, the pupils will not reflect the infrared (IR) illumination directly back into the camera, thus reducing the brightness of the pupil images

- The subject's eyeglasses can sometimes block the reflection from the pupils, resulting in a failure to detect the eyes

- Jewelry and metal framed eye-glasses can reflect strong external illumination and cause a false detection of the pupils

- Different eye colors can cause variable contrast in the iris area, and these variations can affect the threshold setting and cause detection failure

The analysis that follows was conducted after the fact, using data collected at another facility using a simple experimental set up. The subjects were photographed with a single camera equipped with a single IR illuminator. The IR illumination was constant for each frame. Alternative approaches to addressing the above problems exist, but require more sophisticated systems for the initial data collection. For example, according to Zhu and Ji [4], the most effective way to remove false detections due to background clutter (eyeglasses and jewelry) is to compute the image difference between two alternate IR illuminations: one that is on-axis and one that is off-axis. These consecutive images are captured in alternate camera frames. The on-axis IR illumination produces a strong reflection from the pupils, while the off-axis IR illumination results in a weak reflection.

Manuscript approved October 29, 2009.

Assuming that the background does not change dramatically between these two IR illuminated images, computing the image difference will remove some of the false pupil detections caused by background variation.

Since our goal is to achieve real-time detection, algorithms that are too complicated or require a long processing time are unsuitable. Similarly, due to the limited number of available subjects, the training based pattern recognition methods for eye detection are also inapplicable. In the following sections, the algorithm that we developed for detecting and tracking the pupils is described.

2) Approach

Figure 1 shows the data flow diagram of the new pupil detection and tracking algorithm. First, we read in an infrared image, as shown in Figure 2. Then the infrared image is converted into a gray scale image, as shown in Figure 3. Most morphological filters require gray scale imagery data.

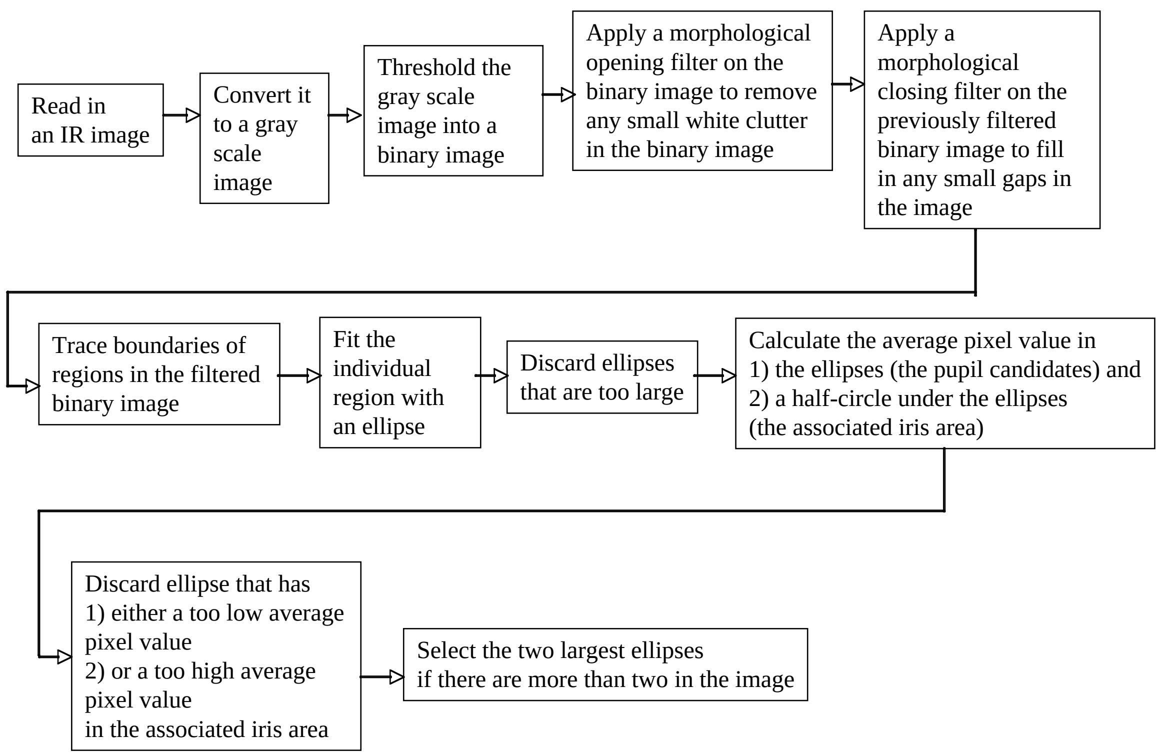

Figure 1 - Data flow diagram of pupil detection

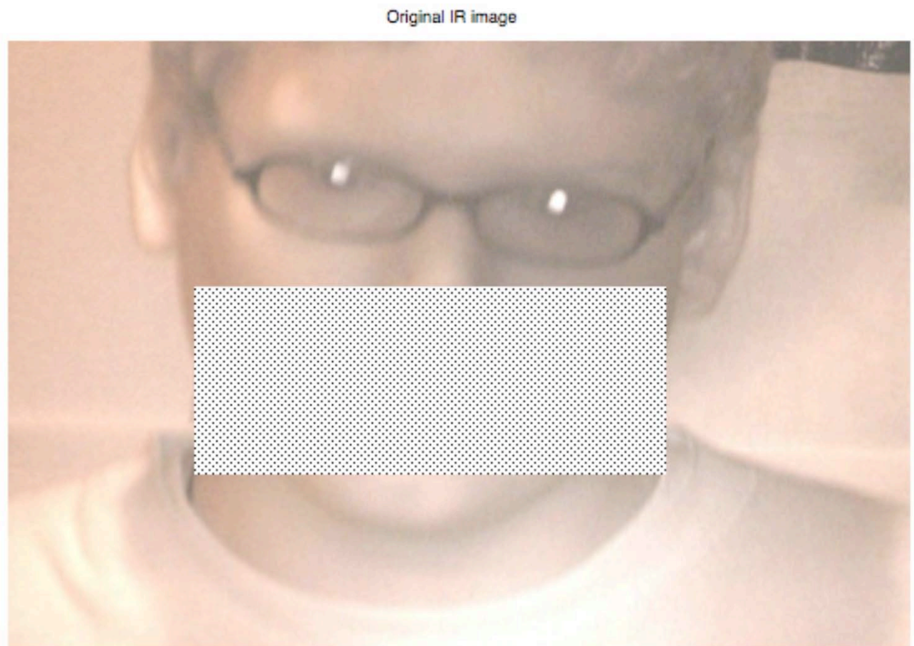

Figure 2 – An original infrared image.

Figure 3 – The gray version of the original image.

a) Thresholding

The gray scale image is thresholded with a properly selected threshold value. The selected threshold value is 204 (80% of the white level). The resultant binary image of the thresholding process is shown in Figure 4. This figure shows several bright areas above the threshold value: two pupils, one earlobe, the chin, two bright patches between the earlobe and the right pupil, the white shirt and some bright patches of background.

It is well established in image processing that too low a threshold value may generate too many false detections while too high a threshold value may prevent some true (correct) detections. Properly choosing a viable threshold value is a key issue. There are different threshold algorithms [5]. Some are based on clustering criteria, some on histogram equalization, some on image entropy, and some on object attributes. A threshold method based on a computationally-inexpensive histogram equalization was tested, but this method did not seem to be very effective. Therefore, a simple hard-threshold method is adopted here. Due to the varying lighting conditions for different subjects, the latter method does not always perform as well as desired. The best working threshold value for individual subject and lighting condition was selected by trial and error. Further investigation is needed to identify which method will be the best for automatic image thresholding, given variable lighting conditions across subjects.

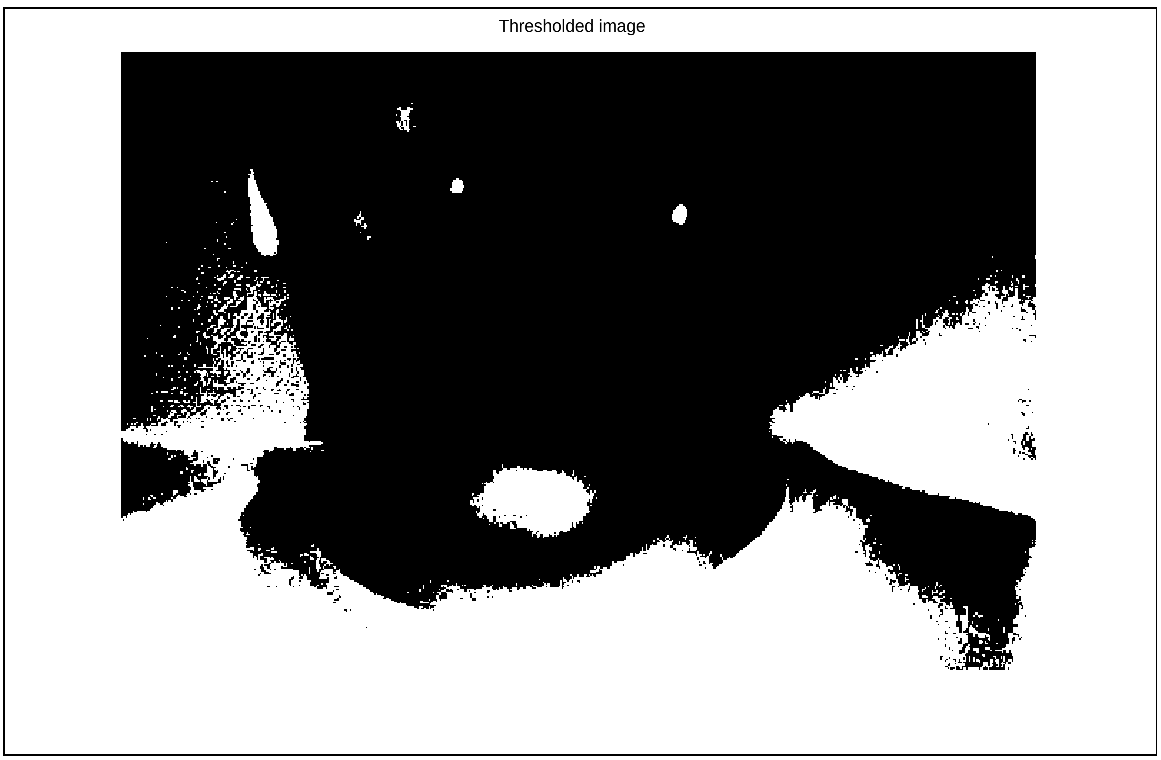

Figure 4 - A resultant binary image after the thresholding.

b) Morphological filtering

We will next apply morphological filters [6] to the thresholded binary image. There are three consecutive stages of morphological filtering: 1) opening, 2) closing, and 3) boundary detection.

We use the morphological opening filter to remove any small objects from an image, while preserving the shape and size of the larger objects present. In essence, the morphological opening is used to remove small white dots in the image. A resultant image is shown in Figure 5. Comparing this figure with Figure 4, notice that most of the small white dots are removed.

We then apply the morphological closing filter to fill small gaps in the larger objects in the image, while preserving the shape and size of these objects. In essence, the morphological closing filter is used to fill the small black spots in the image with white pixel values. This procedure also smoothes the edges of the large objects in the image. A resultant image is shown in Figure 6. Comparing this figure with Figure 5, notice that many of the small black holes are filled with white pixel values.

In the third step of morphological filtering, we apply the boundary detector to trace the exterior boundaries of objects, as well as the boundaries of the holes inside of these objects, within the binary image. A resultant image is shown in Figure 7. In this image, the detected boundaries are overlaid on the original infrared image. There are eight objects in total: two pupils, one earlobe, two small white patches between the earlobe and the right eye, the chin, the white shirt merged with a bright background patch just above the right shoulder and the bright background patch just above the left shoulder.

All of the morphological filter operations are associated with a ’structure element‘ that defines the size of an operation kernel, and different sizes of the structure element can produce slightly different operational results. Some trial and error is required to find the proper size for the structure element.

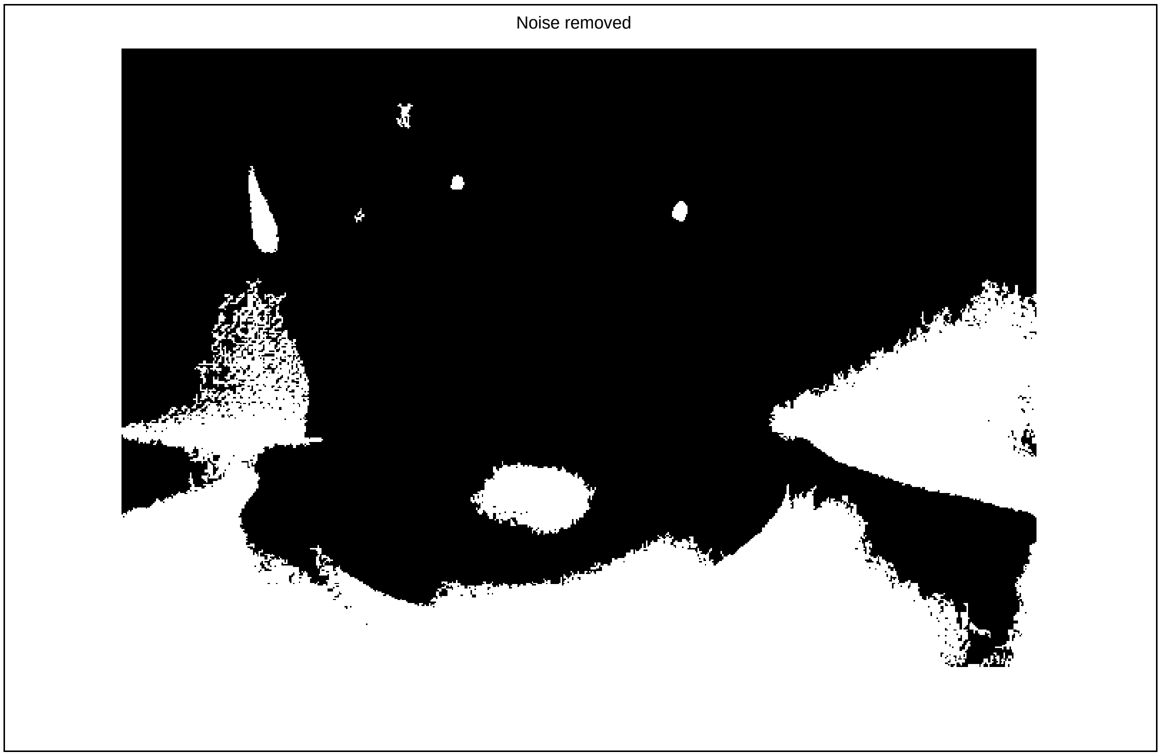

Figure 5 – A resultant image after the morphological opening process.

Figure 6 – A resultant image after the morphological closing process.

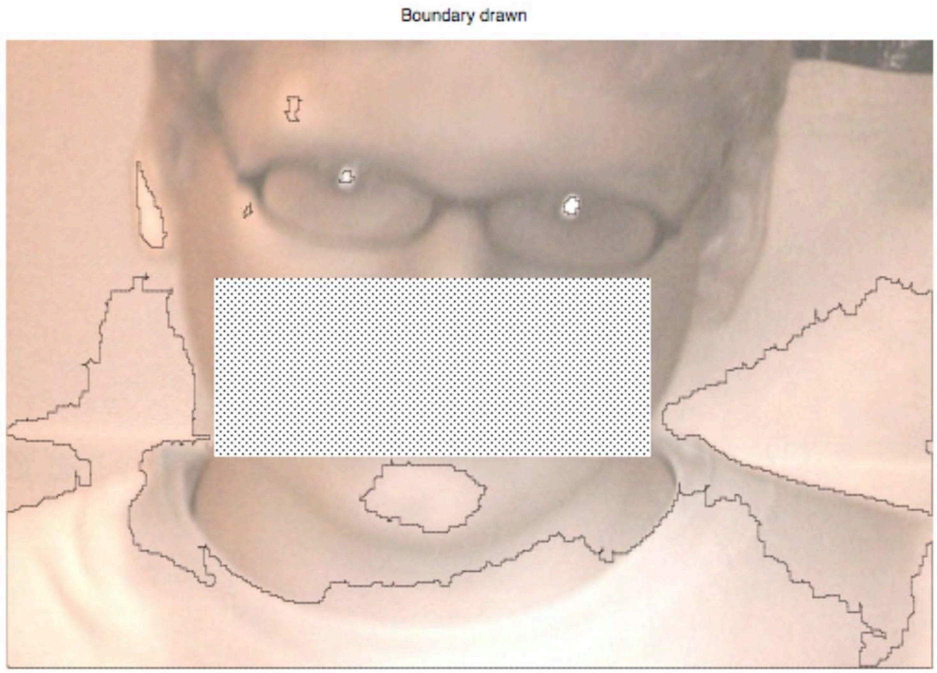

Figure 7 – The detected boundaries overlaid on the original infrared image.

c) Fitting the detected objects with ellipses

After detecting the constituent objects using morphological filtering, it is necessary to fit the objects with ellipses. Some researchers [7, 8] propose fitting the detected objects with circles, because the pupil itself is circular. Alternatively, Z. Zhu and Q. Ji [9] proposed using ellipses to fit the detected objects.

Initially, we fitted the detected objects with circles. We did achieve some good results, but circular fitting always failed when the subject presented with head motion. After further investigation, we concluded that fitting the detected pupils with a circle works only when there is no head motion by the subject. When the subject does initiate head movement, the pupil will appear as a streak, rather than as a circle, due to the high-speed movement of the eye relative to the digital sampling speed of the camera. Fitting the streak of a pupil with a circle often resulted in failure to detect the pupil at all. In Figure 8 a circle was successfully fitted to one elongated pupil, but not to the other. Figure 9 shows two ellipses successfully fitted to both elongated pupils.

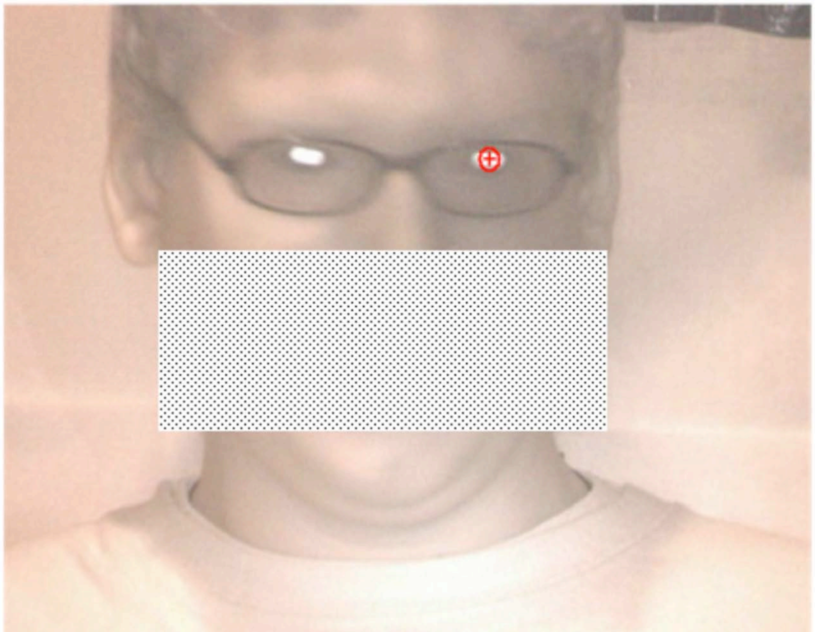

Figure 8 –Fitting the elongated pupils with circles often failed.

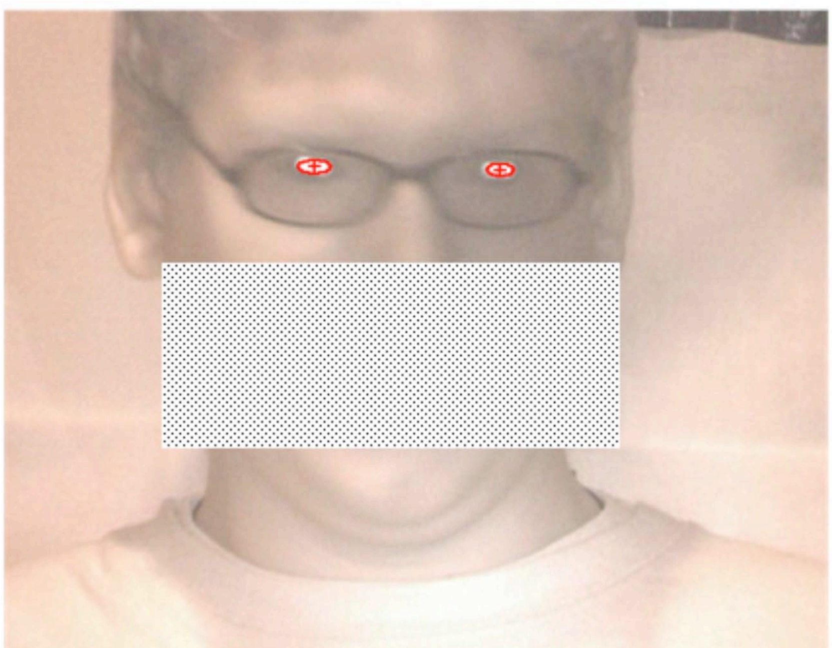

Figure 9 – Fitting the elongated pupils with ellipses had a higher successful rate of pupil detection rate.

After recognizing this sampling issue, the circle fitting was replaced with ellipse fitting. This modified algorithm improves the pupil detection quite dramatically. Figure 10 shows the detected objects with fitted ellipses. The size of ellipse can affect the outcome. The maximum size of the ellipse is set to be 255 pixels in this example; therefore, any object that has a greater size than 255 pixels is removed. In Figure 7, the largest white area is the white shirt merged with a bright spot just above the right shoulder of the subject. This artifact is eliminated in Figure 10. By applying the “constraint of ellipse size“, unwanted ellipses may be removed.

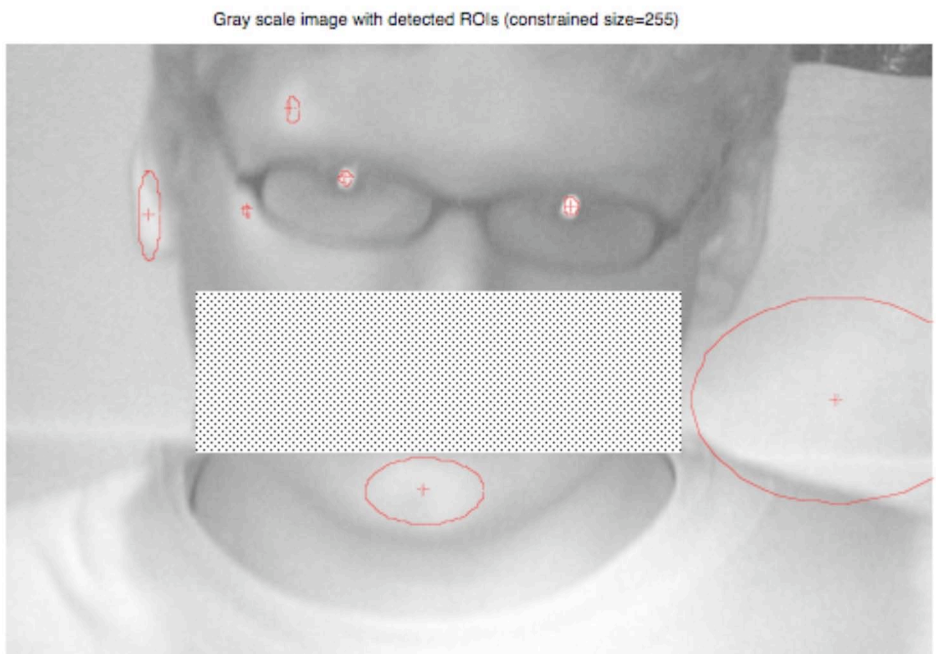

Figure 10 – Detected ellipses overlaid on the gray scale image.

We can also reduce the size of the ellipse to approximate the size of pupil in the image. This will eliminate detection of the earlobe, the chin and the bright spot just above the left shoulder. The results of fitting these objects with a smaller ellipse are shown in Figure 11. Here, the size of ellipse is further reduced to 14 pixels.

d) Add image intensity constraints on the detected ellipse

With a smaller size ellipse (i.e., no larger than 14 pixels), we can eliminate the false detection due to the earlobe, the chin, and the bright background patch just above the left shoulder as shown in Figure 9. Nonetheless, there are some false detections remaining; for example, the two bright spots between the earlobe and the right eye. The next question is - how can we eliminate false detections that satisfy the same size criteria as the real pupil? The answer lies in applying the “constraints of local image intensity”.

We observe that the associated iris area is usually darker than the pupil, while a bright spot that is a false detection does not have a comparable dark area adjacent to it. A lower half circle with a diameter proportional to the pupil size is use to model the iris area adjacent to a potential pupil. The green half circles in Figure 11 shows the postulated iris area superimposed on the candidate pupil detections.

The average pixel value of the pupil and its associated iris area are calculated for each potential pupil. These two pixel average values are compared against their corresponding threshold value. A potential pupil identification will be discarded if the average pixel value of the pupil is too low or if the average pixel value of the associated iris area is too high. This local image intensity thresholding method is an application of the “constraints of local image intensity”.

It is observed that different subjects may have different average pixel values for their iris area due to different eye colors. Therefore, the threshold value for the average pupil and the iris area is obtained by trial and error. The final detection result is shown in Figure 12. Here, the detected pupils are overlaid on the original infrared image.

Figure 11 – The detected small ellipse with associated iris area.

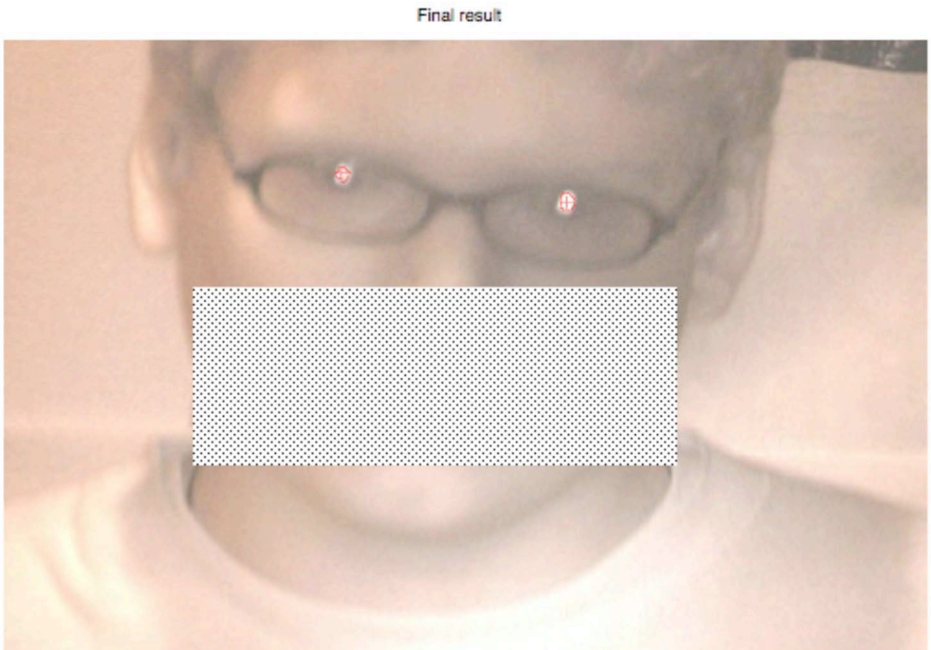

Figure 12 – The final detected pupils are overlaid on the original IR image.

3) Conclusion and Discussion

We have demonstrated the success of a morphological filtering approach on pupil detection. There are some issues however, requiring further investigation before a fully automatic system can be realized. Specifically, the selection of different threshold values is based on trial and error. We would need to develop automatic approaches for normalizing: 1) the image intensity, 2) the average size of human pupil, and 3) the average pixel value for an iris area with different eye colors. In addition, it is possible that false detections may pass through the "ellipse size constraint" and the "local image intensity constraint" described here. Removing these false detections remains a challenging problem.

Regarding data collection, the errors in the pupil detection process may be aided by consistently using the same geometry of subject, lighting source, and camera, as well as the same lighting intensity. Additionally, control of reflections that may cause false alarms is also desirable, perhaps by having jewelry removed and darker clothing worn by subjects.

4) Acknowledgments

We would like to thank Dr. Ruth Willis for her support on this project without which it would have been impossible to pursue this research. We would also like to thank Dr. James Ballas and Dr. Joseph Collins for their helpful discussions on the data analysis, and Mr. Frank Segaria for his assistance in image data preparation.

5) References

[1] B. M. Depaulo, J. J. Lindsay, B. E. Malone, L. Muhlenbruck, K. Charlton, and H. Cooper, "Cues to Deception", *Psychological Bulletin*, Vol. 129, No. 1, pp. 74-118, 2003.

[2] S. Mann, A. Vrij, and R. Bull. "Suspects, Lies, and Videotape: An Analysis of Authentic High-Stake Liars", *Law and Human Behavior*, Vol. 26, No. 3. pp. 365-376, 2002.

[3] O. Tuisku, R. Bates, O. Stepankova, M. Fejtova, P. Novak, H. Istance, F. Corno, and P. Majaranta, (2008) D2.6. "A survey of existing 'de-facto' standards and systems of gaze based mobility control." *Communication by Gaze Interaction (COGAIN)*, IST-2003-511598: Deliverable 2.6.

[4] Z. Zhu and Q. Ji, "Robust real-time eye detection and tracking under variable lighting conditions and various face orientation", *Computer Vision and Image Understanding*, Vol. 98, Issue 1, pp. 124-154, April 2005.

[5] M. Sezgin and B. Sankur, "Survey over image thresholding techniques and quantitative performance evaluation", *Journal of Electronic Imaging*, Vol. 13, No. 1, pp. 146–165, 2004.

[6] P. Soille, *Morphological Image Analysis*, Springer-Verlag, Berlin, 1999.

[7] K.M, Lam and H. Yan, "Locating and extracting the eye in human face images", *Pattern Recognition*, Vol. 29, No. 5, pp. 771-779, 1996.

[8] X. Xie, R. Shudhkar, and H. Zhuang, " On improving eye feature extraction using deformable templates', *Pattern Recognition*, Vol. 27, Bo. 6, pp. 791-799, 1994.

[9] Z. Zhu and Q. Ji, "Robust real-time eye detection and tracking under variable lighting conditions and various face orientations", *Computer Vision and Image Understanding*, Vol. 98, Issue 1, pp.124-154, April, 2005.